APPLIED ORGANOMETALLIC CHEMISTRY, VOL. 7, 381–389 (1993)

Si/C/F/H materials from laser-explosive decomposition of fluoromethylsilanes

J. Pola,*[a] Z. Bastl,*[b] J. Tláskal,*[c] H. Beckers,† H. Bürger,† P. Moritz† P. Weiss‡ and M. Sigrist‡

* Academy of Sciences of Czech Republic ([a] Institute of Chemical Process Fundamentals, 165 02 Prague 6 Rozvojova str. 135; [b] J. Heyrovský Institute of Physical Chemistry and Electrochemistry, 182 23 Prague 8; [c] Institute of Inorganic Chemistry, 25 068 Řež, near Prague, Czech Republic), † Anorganische Chemie, FB 9, Universitat-GH, W-5600 Wuppertal 1, Germany, and ‡ Institute of Quantum Electronics, ETH, 8093 Zurich, Switzerland

Solid Si/C/H/F materials laser-deposited from gaseous fluoro-methylsilanes are examined by XPS, SEM, IR and Raman spectroscopy and revealed to be a blend of silicon–carbon-based frameworks, possessing some Si–H and C–H bonds, and carbon whose modification is dependent on the structure of the parent fluoromethylsilane. Their properties are affected by contact with the atmosphere: although incorporation of oxygen into silicon–carbon frameworks is a very fast process, the dramatically improved adhesion to aluminium requires long exposure periods.

Keywords: Si/C/H/F materials, laser deposition, laser spallation, structure, reactivity

INTRODUCTION

Chemical vapour deposition (CVD) from organosilanes[1–6] is a recognized technique for production of materials with promise in various practical applications. One application of laser-induced CVD processes relates to deposition of organosilicon polymers and sinterable powders. The polymers have been deposited by infrared laser photosensitized homogeneous decomposition of silacyclobutanes,[7–11] silacyclohexane[12] and some oxygenated organosilanes,[13] by excimer laser photolysis of hexamethyldisilazane,[14] and by infrared laser evaporation of polycarbosilane.[15] Sinterable powders were produced by excimer laser photolysis of chloromethylsilanes[16] and by infrared laser decomposition of hexamethyldisilazane, hexamethyldisiloxane,[17,18] tetramethylsilane and hexamethyldisilane.[19]

We have recently reported[20,21] on a CO_2 laser induced explosive decompositon (LID) of fluoromethylsilanes $F_nH_{3-n}CSiH_3$ [**I** ($n=1$), **II** ($n=2$) and **III** ($n=3$)] and $(F_3C)_2SiH_2$ (**IV**) which affords a variety of volatile products and furnishes different Si/C/F/H materials, and discussed its gas-phase chemistry and an efficient reduction of the strong C–F bond. Chemical reactions involved during a single-pulse of the laser radiation were judged to be initiated by a dyotropic rearrangement for **I** (Eqn [1]) and by a series of carbene cleavage/insertion reactions in the case of **II–IV** (Eqn [2]).

$$FCH_2—SiH_3 \rightarrow H_3C—SiH_2F \qquad [1]$$

$$H_nCF_{3-n}—SiH_3 \rightarrow [H_nCF_{2-n}: + FSiH_3] \rightarrow H_{n+1}CF_{2-n}—SiH_2F \qquad [2]$$

These reactions were followed by further steps differing in their extent with the particular fluoromethylsilanes and shown to afford methane, ethyne, trifluorosilane and tetrafluorosilane. Methane was inferred to be formed from precursors with a CH_3Si group, while ethyne and fluorosilanes were supposed[21] to arise via a sequence of reactions of intermediary fluorovinylsilanes (Eqn [3]) and ethynylsilanes (Eqn [4]).

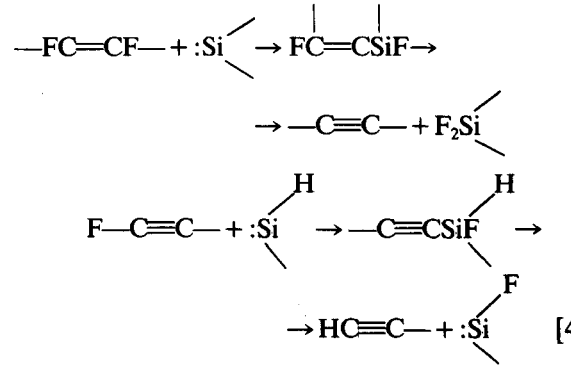

[3]

[4]

0268–2605/93/060381–09 $09.50

Received 19 April 1993
Accepted 1 July 1993

This ensures a complete and irreversible SiH–SiF exchange and formation of C_2H_2.

This paper concentrates on the properties of the materials deposited in the above processes; these properties are studied by using ESCA and EDX–SEM techniques, and it correlates these properties with the chemical processes in the gas phase through which the materials are formed.

EXPERIMENTAL

The technique of CO_2 laser irradiation of the fluoromethylsilanes **I–IV**, including the description of the reactor equipped with NaCl windows, is given in a previous paper.[21]

IR spectra of the deposits on NaCl windows were measured after evacuation of the reactor. Raman spectra of the solids were measured at room temperature using the 514.5 nm line of an Ar^+ laser for excitation.

In order to evaluate the properties of deposits by ESCA and SEM analyses, deposits were produced on aluminium sheets housed in the reactor before irradiation. X-ray photoelectron spectra (XPS) were measured on a VG ESCA 3 Mk II electron spectrometer using Al Kα achromatic radiation ($h\nu = 1486.6$ eV). The spectrometer was operated in fixed-analyser transmission mode. Detailed scans were taken over carbon 1*s*, silicon 2*p*, oxygen 1*s* and fluorine 1*s* regions. The background pressure of residual gases during spectrum accumulation was typically 10^{-6} Pa. Core level binding energies were determined with an accuracy ± 0.2 eV. The XPS peak positions and areas were determined by fitting the unsmoothed experimental data after subtracting the linear background. Theoretical photoionization cross-sections[22] and mean free electron paths calculated from the equations suggested by Seah and Dench[23] were used to convert peak areas into the elemental concentrations. The samples were exposed to the ambient atmosphere during their transport from the reactor to the electron spectrometer.

Scanning electron microscopy studies of the deposit were performed on an ultrahigh-vacuum instrument (Tesla BS 350) equipped with an energy-dispersive analyser of X-ray radiation (Edax 9100/65). An ECON detector in the 'shield mode' (plastic window) was used for the qualitative determination of light elements (carbon, oxygen, fluorine). The morphology of samples was usually investigated using an accelerating voltage of 16 kV. Analyses of thin layers for the determination of light elements were carried out using an accelerating voltage of 4 kV. Specimens were fixed by Leit-C-plast and analysed after sputtering a silver layer of about 20 nm onto the samples.

Laser spallation experiments[24] with the materials deposited on aluminium substrates were carried out by irradiating the substrate with a Nd:YAG laser (wavelength 532 nm, pulse duration 7 ns, pulse energy 10–100 mJ). The spots of the deposits opposite substrate areas exposed to the laser pulses were first examined using a microscope and then analysed by EDX–SEM spectroscopy in order to compare the elemental composition of the deposit areas before and after spallation.

RESULTS AND DISCUSSION

Spectral analyses

The data on the solid deposits obtained by single-pulse LID of fluoromethylsilanes **I–IV** are given in Table 1 and Figs 1 and 2. Various views on their composition can be acquired by applying different analytical techniques: therefore, ECSA, SEM, IR and Raman spectroscopic data need to be considered as complementary to one another in order to obtain a true picture of the composition and bonding character of the solid materials. We remark that ESCA analyses provide information on superficial (up to 5 nm) layers only, while EDX–SEM data give an insight into depths up to almost 0.3 μm. We also note that the EDX–SEM analysis of the aluminium substrate (Fig. 1f) is compatible with minor impurities of carbon and oxygen. However, amounts of these elements are too low to invalidate the following assumptions on EDX–SEM analyses of the deposits.

Deposit from I

The IR spectrum of the solid (a broad band between 800 and 900 cm^{-1}) is very similar to that of silicon carbide[25] and it proves the occurrence of some material with many Si–C and some with few Si–H and C–H bonds. The Raman absorption is typical[26] of amorphous carbon. ESCA analyses are consistent with the concentration of carbon and silicon about seven times higher than that of

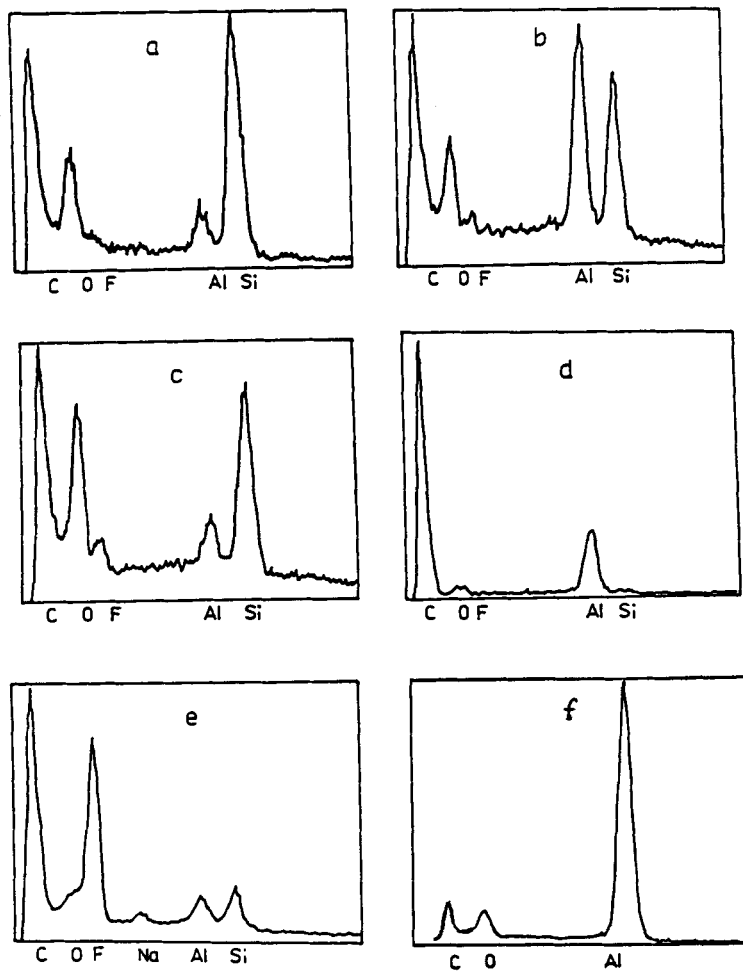

Figure 1 EDX-SEM analysis of the deposits from LID of **I–IV** (in a–d, respectively, on Al) and **IV** (e, on NaCl); f, Al substrate.

fluorine and with the presence of a significant amount of oxygen. Both carbon and silicon are present in two chemically inequivalent forms differing in carbon 1 *s* and silicon 2*p* electron binding energies by 1.6 and 2.2 eV, respectively. The forms of the lower values of the core level binding energy prevail, and their relative abundance, obtained by curve fitting of the recorded spectra, amounts to 65% for carbon and 75% for silicon. Comparison of the measured binding energies with the published[27,28] values, indicates that a greater part of silicon is incorporated into an organosilicon compound, while less of it is likely bonded to fluorine or oxygen. In order to find out whether silicon carbide is also present in the deposit, we have measured a reference sample of silicon carbide (SiC) and observed core level binding energies equal to 100.4 ± 0.3 eV for silicon 2*p* electrons and 282.5 ± 0.2 eV for carbon 1 *s* electrons. As photoemission lines with these values of binding energies were absent in the spectra of the deposits, the presence of silicon carbide can be excluded. On the basis of similar considerations, we can also rule out the presence of C–F bonds. Qualitative EDX analyses (Fig. 1a) reveal significant amounts of silicon and also of carbon, which are accompanied by some oxygen. An SEM image of the deposit morphology, illustrated in Fig. 2(a), reveals dark compact material overlaid with a light woven texture.

Deposit from II

This can be obtained[21] in a noticeable amount only at relatively higher pressures, since LID at 3 kPa results in only a translucent layer the IR spectrum of which indicates the presence of hydrogenated amorphous silicon[29–31] and of SiF_6^{2-} ($725\ cm^{-1}$). The IR spectrum of the deposit pro-

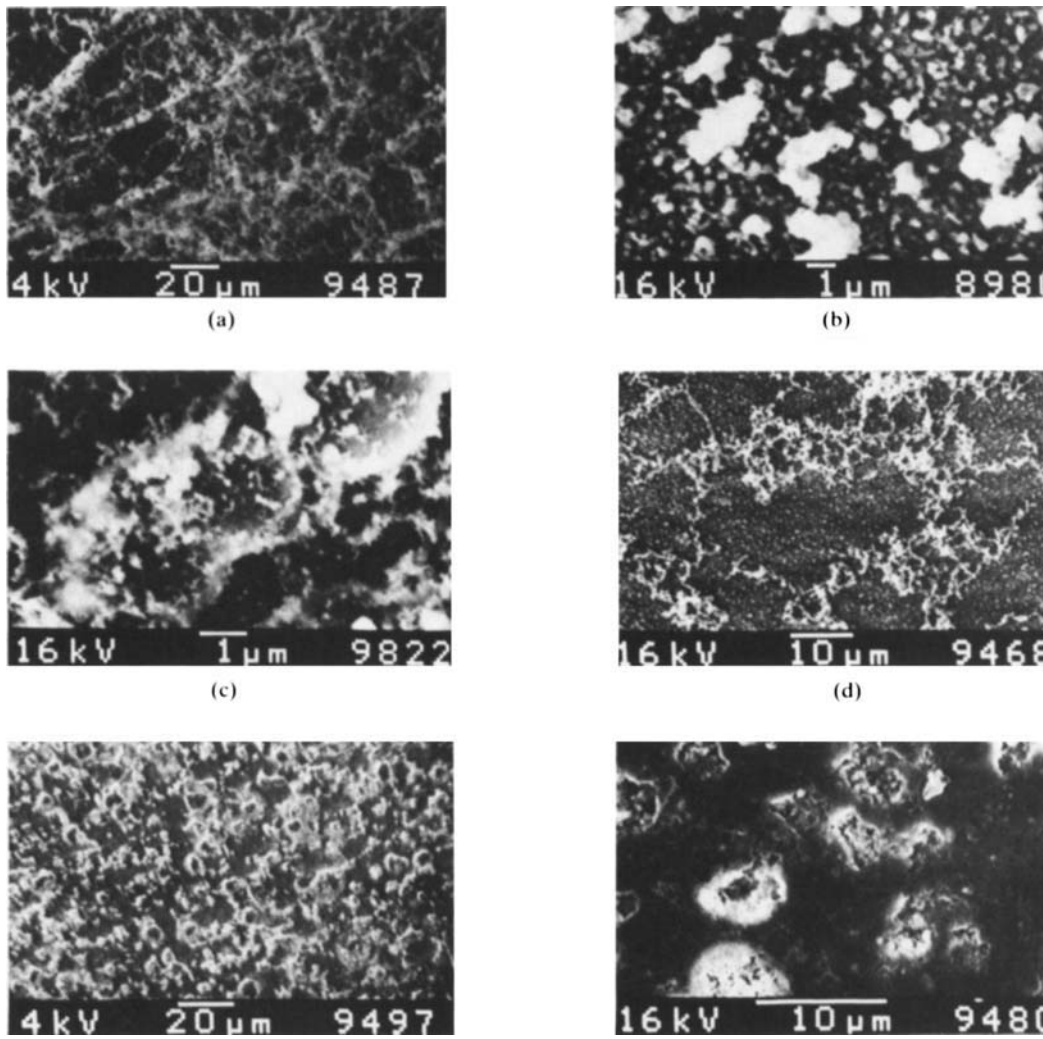

Figure 2 SEM images of deposits from LID of **I** (a), **II** (b, 3 kPa; c, 5.3 kPa), **III** (d) and **IV** (e, on Al; f, on NaCl).

duced at higher pressure is different: it is in accord with a material rich in Si–C but poor in Si–H and C–H bonds.

The ESCA analysis of the deposit obtained at the higher pressure incorporates almost equal amounts of carbon and oxygen, less silicon and very little fluorine. The widths and asymmetry of silicon 2*p* (and carbon 1*s*) peaks suggest that the peaks are composed of at least two lines. The silicon 2*p* spectra were fitted with two Gaussian–Lorentzian peaks of equal widths. The silicon 2*p* lines could be deconvoluted into more components, but their assignment based on available literature data[32,33] would be rather uncertain unless measurements of core level binding energies on well-defined standards were taken. The separation of the silicon 2*p* lines deduced by curve fitting of the spectra was 2.0 ± 0.1 eV. A comparable separation of carbon 1*s* peaks was observed. The lower binding energy of silicon 2*p* and carbon 1*s* lines can be attributed to Si–C bonds, probably from silicon carbide. The higher binding energy of the silicon 2*p* component is associated with the presence of tetravalent silicon. On the basis of a comparison with literature data,[32] a fluorine 1*s* binding energy of 687.5 eV has been assigned to silicon oxyfluorides.

A qualitative EDX analysis (Fig.1b) of the

deposits obtained at lower and higher pressures reveals the presence of silicon and carbon, and also of oxygen accompanied by small amounts of fluorine. An SEM image of the deposits reveals the occurrence of agglomerates whose size ranges from less than 1 μm at the lower pressure (Fig. 2b) to more than 10 μm in the higher-pressure experiment (Fig. 2c).

Deposit from III

The IR spectrum reveals the presence of SiF_6^{2-} and also that of Si–C and C–H bonds. A broad absorption band can be assigned to the ν(Si–C) mode of silicon carbide with possible contributions from ν(Si–F) and/or $\delta(SiH_2)$ modes.

The composition of superficial layers analysed by ESCA reveals twice as much carbon as silicon, a variable and important content of oxygen and a low concentration of fluorine. This corresponds to the pattern of the composition of a thicker sample obtained by EDX–SEM analysis (Fig. 2c) and it does not give any evidence for elemental silicon. The silicon 2*p* spectra do not suggest the presence of more than one form of silicon. The binding energy value (103.1 ± 0.2 eV) is consistent with that found for tetravalent silicon bonded to oxygen. The carbon 1*s* spectra exhibit asymmetry as a shoulder at higher binding energy, which is characteristic of graphitic carbon. Alternatively, the carbon 1*s* line shape can be interpreted as being caused by the presence of small amounts of carbon atoms with higher binding energies due to their bonding to oxygen.[28]

SEM morphology images (Fig. 1d) are in line with compact black material covered with white particles. We presume that this compact material consists of carbon, whilst the white separated agglomerates are organosilicon polymers. Their discontinuous structure implies that they do not recombine while they are being deposited.

Deposit from IV

This is inferred, on the basis of the material balance,[21] to be composed mostly of carbon. Indeed, the Raman spectrum of the deposit can be correlated[34] with the vibrational spectrum of graphite. The IR spectrum implies the presence of some C–H but not Si–H bonds. Na_2SiF_6 is indicated as well. The analysis by ESCA reveals the preponderance of carbon and some content of oxygen, silicon and fluorine. The silicon is present in two forms differing by 1.3–1.4 eV in the silicon 2*p* binding energy. Both silicon-containing species are approximately equally abundant. The silicon with the lower binding energy is probably bonded to carbon while that with the higher binding energy (103.4–103.7 eV) corresponds to tetravalent silicon bonded to oxygen. The carbon 1*s* line exhibits a satellite, relative intensity 15% of the main line, with a binding energy 3.6 eV higher than that of the parent line. This may correspond to carbon in —C=O or —COO groups.[28]

The qualitative EDX analysis shows carbon with very little oxygen (Fig. 1d). Carbon, fluorine, some silicon and little oxygen are found on the NaCl window (Fig. 2e). The morphology of the deposit on the two different substrates (aluminium and NaCl, Figs 2e, f) differs as well, a light network texture being observed on aluminium, while a light, bulkier, island structure appears on NaCl. More silicon and a greater content of lighter aggregates on NaCl support the conclusion that the light particles contain silicon.

Structure and formation of the deposit

The ESCA results on the superficial layers (Table 1, Fig. 3), along with the EDX–SEM data of the bulk material (Fig. 1), reveal that the deposits from **I–III** are somewhat similar regarding their composition and in possessing a significant content of Si–C frameworks which incorporate some C–H and Si–H bonds. These frameworks are compounded with amorphous carbon (**I**), silicon carbide (**II**) and graphite (**III**). Fluorine, being present in all these deposits in very small amounts, can be judged as bonded to silicon, which experiences at least two different forms: in one of these, silicon appears to be bonded only to carbon, while in another it is also linked to oxygen and/or fluorine. Elemental silicon has never been detected. Oxygen, which is absent in the precursors **I–IV**, must have become incorporated by contact of the materials with air. The deposits were shown to contain some oxygen immediately after their formation and this cannot be ascribed only to contact with air during their transport from the reactor, but must be due to some very small leakage of air into the reactor. This extremely high sensitivity of the silicon laser deposited materials towards oxidation has also been observed in Refs 19 and 35, but it cannot be compared with a relatively slow ageing process of plasma-deposited silicon-containing films described in Ref. 3. The high reactivity can obviously be related to fast reactions with oxygen of unsaturated carbon and/or silicon centres of the

Table 1 Data on deposits in LID of fluoromethylsilanes **I–IV**

Fluoromethylsilane	Pressure (kPa)	ESCA analysis	IR spectrum, (cm^{-1})	Raman spectrum[a] (cm^{-1})
I	4	$C_{2.0}O_{0.9}Si_{2.0}F_{0.3}$	800–900 (vs), 2160 2850, 2930, 3000 (all w)	1500
II	3		725 (vs), 650, 840–900, 2150–2250 (all w)	
II	5.3	$C_{2.0}O_{2.2}Si_{1.5}F_{0.3}$	850, 940 (both vs), 1100, 2150, 2900 (all w)	
III	4	$C_{2.0}O_{1.5-2.0}Si_{1.1}F_{0.2}$	725 (vs), 910, 960 (both vs), 2150, 2950 (both w)	
IV	4	$C_{2.0}O_{0.16-0.4}Si_{0.1}F_{0.10-0.25}$	925 (vs), 2950 (w)	1300, 1600

[a] Ref. 21.

silicon–carbon frameworks. The observation that oxygen is linked to both silicon and carbon suggests that these bonds can be formed, apart from other possibilities, by the addition of oxygen (O_2) across an unsaturated bond between silicon and carbon[36] (Eqn [5]).

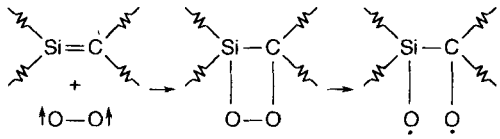

[5]

A high content of oxygen is found in these deposits, which are rich in silicon, but there is a very small oxygen content in the deposit from **IV**, wherein silicon is almost absent; this indicates that silicon provides a route for oxygen incorporation. We presume that the unsaturated nature of the deposited agglomerates is a property which is worthy of further studies, especially from the point of view of chemical reactions of these particles with other reactive molecules.

We deduce that the main reaction producing the deposits is polymerization of unsaturated alkenyl- and alkynyl-silanes (Eqn [6]):

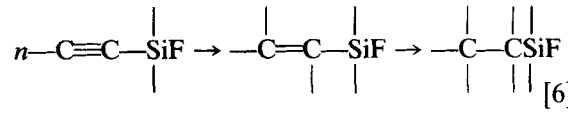

[6]

The low content of Si–H and C–H bonds in the SiC frameworks suggests that this polymerization is accompanied by the additions of silylenes across the double bonds of alkenyl- and alkynyl-silanes and/or by the same additions of carbon- and silicon-centred radicals produced via cleavage of the Si–C bonds of compounds taking part in reactions [1] and [2], and that the adducts formed undergo dehydrofluorination. The high exothermicity of the primary steps (Eqns [1], [2]) and the likelihood of formation of hot products in these additions, make dehydrofluorination feasible and

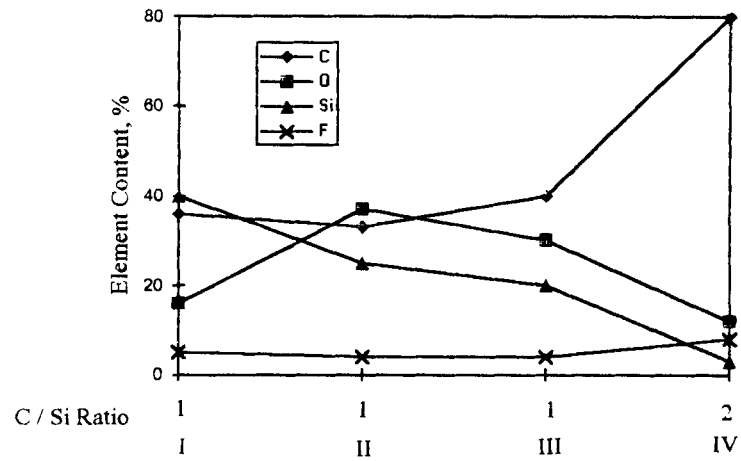

Figure 3 Composition of the deposits obtained by LID of **I–IV**.

can account for a low content of hydrogen and fluorine and a high content of silicon and carbon. In agreement with this suggestion, complete dehydrofluorination of these polymers produces silicon carbide, contained in the deposit obtained from **II**. An alternative reaction leading to Si–H structures via silylene polymerization/dehydrogenation[37] does not seem probable, since it should inevitably result in Si^0, which has not been detected.

The formation of graphite and amorphous carbon takes place via silicon-free or silicon-containing unsaturates and their dehydrofluorination and defluorosilylation (Eqn [7]), since monofluoro-[38] and in particular difluoro-ethyne[39] are suitable precursors for the deposition of carbon, and so it is reasonable to suppose that fluoroethynylsilanes will also be precursors for this deposition.

$$C_2X_2F_2 \xrightarrow[-XF]{} FC{\equiv}CX \xrightarrow[-XF]{} 2C + FX \qquad [7]$$

$$(X = H, Si{\equiv})$$

A different route to carbon may be just dehydrogenation of intermediary unsaturates free of silicon, as described in Refs 40 and 41. All these reactions producing carbon are of major importance in LID of **IV**, where the deposit is very poor in silicon–carbon frameworks and consequently in oxygen. The different form of carbon (graphite in LID of **III** and **IV**, and amorphous carbon in that of **I**, which were identified by Raman spectroscopy[21]) presents a query. The major impact on the growth of the particular carbon modification is known[42] to be provided by the precursors' pressure and substrate temperature, but these parameters can be considered very similar in all LID experiments. The amorphous carbon produced from **I**, and the graphite deposited from **III** and **IV**, might then seem to indicate the effect of different gas-phase chemical processes and reflect modes of stripping off hydrogen, fluorine and silicon groups from the silicon–carbon frameworks.

The content of fluorine in all the deposits is roughly the same (Table 1, Fig. 3), but the F/Si ratio in the deposit from **IV** (1–2.5) is well above the value (0.2) observed with the deposits from **I–III**. The high proportion of fluorine in **IV** is highly supportive of fluorine bonded to carbon and of the production of a material at least somewhat resembling graphite fluoride.[43]

The formation of Na_2SiF_6, which is in line[21] with the occurrence of a reaction between HF, SiF_4 and NaCl and is indicated for **II–IV** but not for **I**, is obviously limited to the NaCl window areas of the reactor.

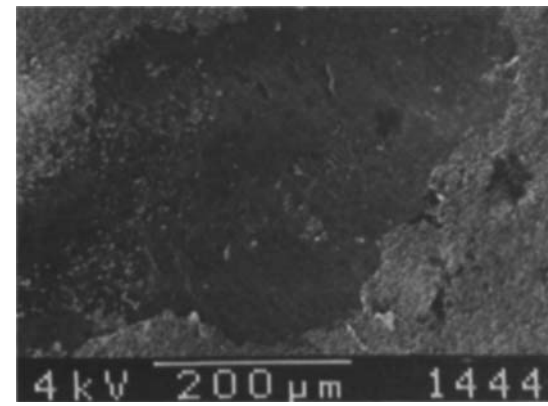

Figure 4 The pattern of spallation achieved with the deposit obtained by LID of **III**.

Adhesion of deposits to aluminium

The deposited layers do not adhere strongly to the surfaces of substrates (quartz, glass, metal) and can be easily mechanically removed. However, their adhesion to metals can be dramatically increased upon a long (several months) exposure to atmosphere. This was indicated for aluminium, when a black layer could not be removed mechanically after prolonged exposure to air. Nd:YAG laser spallation experiments were carried out with deposits from **III** and **IV** in an effort to determine the nature of the increase in adhesion. A typical pattern of an area after spallation and a nearby non-spalled area is illustrated in Fig. 4. The comparison of the EDX traces of the two regions and corresponding morphology patterns are given in Fig. 5. It is revealed that the morphology of both deposits changes somewhat, even after a long contact with air (cf. Figs 2 and 5). The spallation results in a disappearance of the white layer of agglomerates. The EDX analysis shows that the spallation of the deposit from **III** generates a removal of silicon and oxygen (Fig. 5a). On the other hand, no changes in the composition were induced in the spalled spots of the deposit **IV** (Fig. 5b). These data could be explained by assuming that in case (a) the deposits form a layered structure and that the spallation occurred, at the generated stress layers, only partially removing an overlayer of silicon and oxygen without spalling the underlying

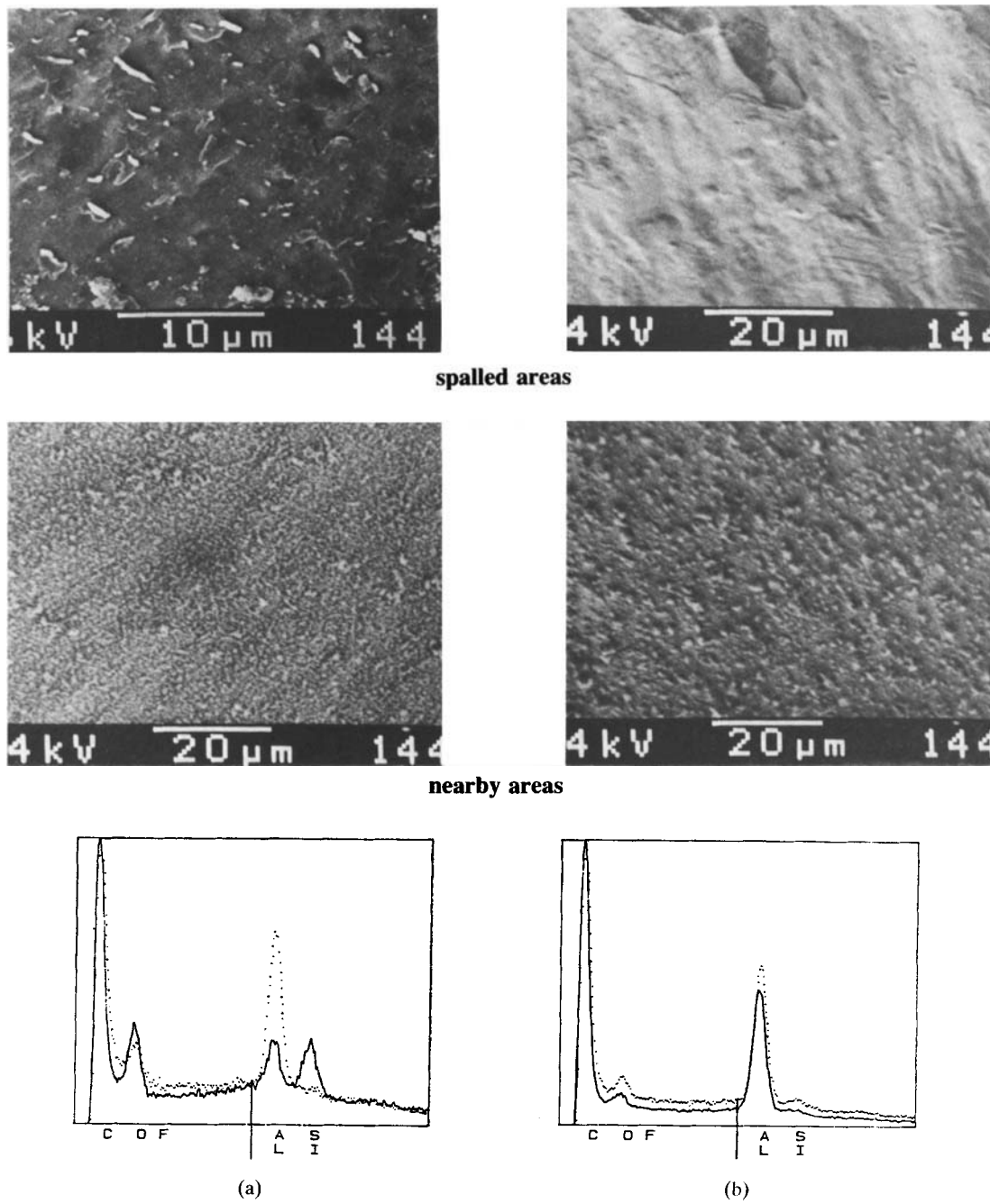

Figure 5 SEM images and EDX–SEM traces of the deposits obtained from LID of **III** (a) and **IV** (b) exposed to long contact with air and spallation. The dotted lines relate to spalled and solid lines to nearby (non-spalled) areas.

carbon film, whereas in case (b) the deposits formed layers of homogeneous composition. This implies that the adhesion of the deposits to the aluminium surface (Al and/or ubiquitous Al_2O_3) can be correlated with a strong interaction between the metal and carbon.

The results suggest that the technique of explosive LID of fluoromethylsilanes can be used as a simple and efficient method for the gas-phase deposition of layers of reactive agglomerates of

poly(carbosilanes), and that these reactive particles might be deliberately modified afterwards by chemical reactions. High adhesion of these polymers compounded with carbon to aluminium, observed upon prolonged exposure to the atmosphere, is worthy of further research, especially if it can be extended to other metals. The reported[21] technique for the laser deposition onto cold substrate surfaces of Si/C/H/F materials which are characterized in this paper can produce advantages over conventional CVD of silicon carbide in practical applications (protective coatings), since the latter method demands very high temperatures.[1] The LID may be also suitable for the deposition of thin photoconductive Si/C/H/F films which are known[44] to be produced in a glow-discharge induced decomposition of mixtures of silane with fluorocarbons.

REFERENCES

1. Schlichting, J *Powder Metall. Int.*, 1980, 12: 141
2. Yasuda, H *Plasma Polymerisation*, Academic Press, Orlando, 1985
3. Wrobel, A M *J. Macromol. Sci.—Chem.*, 1985, A22: 1089
4. Kaloyeros, A E, Corbett, J W, Toscano, P J and Rizk, R B *Mater. Res. Soc. Symp. Proc.*, 1990, 192: 601
5. Horn, M W, Pang, S W and Rothschield, M *J. Vac. Sci. Technol.*, 1990, B8: 1493
6. Gerault, J P, Morancho, R, Constant, G, Mazerolles, P and Manuel, G *J. Anal. Appl. Pyrol.*, 1982, 4: 59
7. Pola, J, Chvalovský, V, Volnina, E A and Guselnikov, L E *J. Organomet. Chem.*, 1988, 341: C13
8. Pola, J, Volnina, E A and Guselnikov, L E *J. Organomet. Chem.*, 1990, 391: 275
9. Pola, J, Čukanová, D, Minárik, M, Lyčka, A and Tláskal, J *J. Organomet. Chem.*, 1992, 426: 23
10. Sedláčkova, M, Pola, J, Volnina, E A and Guselnikov, L E *J. Anal. Appl. Pyrol.*, 1989, 14: 345
11. Čukanová, D and Pola, J *J. Organomet. Chem.*, 1993, 453: 17
12. Urbanová, M and Pola, J *J. Anal. Appl. Pyrol.*, 1993, 24: 325
13. Pola, J, Alexandrescu, R, Morjan, J and Sorescu, D *J. Anal. Appl. Pyrol.*, 1990, 18: 71
14. Pola, J and Taylor, R *J. Organomet. Chem.*, 1993, 446: 131
15. Pola, J, Vítek, J, Polyakov, Yu P, Guselnikov, L E, Matveychev, P M, Bashkirova, S A, Tláskal, J and Bastl, Z *Appl. Organomet. Chem.*, 1991, 5: 57
16. O'Neil, J A, Horsburg, M, Tann, J, Grant, K J and Paul, G L *J. Am. Ceram. Soc.*, 1989, 72: 1130
17. Rice, G W and Woodin, R L *Prog. Soc. Photo-Opt. Instrum. Eng.*, 1984, 458: 98
18. Rice, G W *J. Am. Ceram. Soc.*, 1986, 69: C-183
19. Von Scholz, M, Fuss, W and Kompa, K L *Angew. Chem.*, in press
20. Pola, J, Beckers, H and Bürger, H *Chem. Phys. Lett.*, 1991, 178: 192
21. Pola, J, Bastl, Z, Tláskal, J, Beckers, H, Bürger, H and Moritz, P *Organometallics*, 1993, 12: 171
22. Scofield, J H *J. Electron. Spectrosc. Relat. Phenom.*, 1976, 8: 129
23. Seah, M P and Dench, W *Surf. Interf. Anal.*, 1979, 1: 2
24. Weiss, P and Sigrist, M W in *Photoacoustic and Photothermal Phenomena III*, Bicanic, D (ed), Springer Series in Optical Sciences No. 69, Springer-Verlag, Berlin, 1992, p. 287.
25. Fantoni, R, Borsella, E, Piccirillo, S, Ceccata, R and Enzo, S *J. Mater. Sci.*, 1990, 5: 143
26. Wada, N, Gaczi, P J and Solin, S A *J. Non-Cryst. Solids*, 1980, 35/36: 549
27. Briggs, D and Seah, M P (eds) *Practical Surface Analysis by Auger and X-ray Photoelectron Spectroscopy*, J Wiley, Chichester, 1983, p 488
28. Windawi, H and Ho, F F-P (eds) *Applied Electron Spectroscopy for Chemical Analysis*, J Wiley, New York, 1982, p 105
29. Lucovsky, G, Nemanich, R J and Knights, J C *Phys. Rev.*, 1979, B19: 2064
30. Brodsky, M H, Cardona, M and Cuomo, J J *Phys. Rev.*, 1977, B16: 3556
31. John, P, Odeh, I M, Thomas, M J K, Tricker, M J, Riddoch, F and Wilson, J I B *Philos. Mag.*, 1980, B42: 671
32. Zazzera, L A and Moulder, J F *J. Electrochem. Soc.*, 1989, 136: 484
33. Ermolieff, A, Martin, F, Amoroux, A, Marthon, S and Westendorp, J F M *Appl. Surf. Sci.*, 1991, 48/49: 178, and refs therein
34. Nakamura, K, Fujitsuka, M and Katajima, M *Phys. Rev.*, 1990, B41: 12260
35. Díaz, L, Santos, M, Siguenza, C L, Domingues, P, González-Díaz, P F, Fajgar, R, Bastl, Z, Tláskal, J and Pola, J *J. Chem. Soc., Faraday Trans.*, in press
36. Davidson, I M T, Dean, C E, Lawrence, F T *J. Chem. Soc., Chem. Commun.*, 1981, 52
37. Longeway, P A and Lampe, F W *J. Am. Chem. Soc.*, 1981, 103: 6813
38. Middleton, N J and Sharkey, W H *J. Am. Chem. Soc.*, 1959, 81: 803
39. Bürger, H and Sommer, S *J. Chem. Soc., Chem. Commun.*, 1991, 456
40. Jenkins, G M and Kawamura, K *Polymeric Carbons—Carbon Fibre, Glass and Char*, Cambridge University Press, Cambridge, 1976
41. Kiefer, J H and von Drasek, W A *Int. J. Chem. Kinet.* 1990, 22: 747
42. Tsai, H and Bogy, D B *J. Vac. Sci. Technol. A*, 1987, 5: 3287
43. Nakajima, T and Watanabe, N *Chem. Technol.*, 1990, 426
44. Morimoto, A, Miura, T, Kumeda, T and Shimizu, M *Jpn. J. Appl. Phys.*, 1983, 22, 908